**Supporting information (SI)**

# Efficient electrocatalysts for biomass quasi-solid-state Li-$O_2$ batteries: porous nanocages with nickel-cobalt-N/C active species

Tie Liu, *[a] Guangwei Zhang [a]

[a] *School of Chemistry and Chemical Engineering, Heze University, Heze 274015, China. E-mail: lime1032@163.com*

## Experimental section

### Materials preparation

Typically, cobalt (II) nitrate hexahydrate (2 mmol) was dissolved ultrasonically in 50 mL of methanol to form a clear purple solution. Next, 50 mL of methanol containing 2-Methylimidazole (2-MeIM, 8 mmol) was added dropwise into the solution above under mild stirring treatment. After continuing stirring for 20 min, the resulting solution was transferred and kept at 25 ºC for 24 hours. The ZIF-67 nanoparticles were then collected by symmetric centrifugation, washed with methanol several times to remove the excess ions and residues, and dried at 80 ºC under vacuum. As for the carbonization, the solid-precursor was kept under an Ar atmosphere for 5 min in a furnace before elevating the temperature, then performed the carbonization at 750 ºC for 3 h with a heating rate of

5 ºC $min^{-1}$. Finally, after washed with 0.5 M $H_2SO_4$ solution to remove unstable metal species, a fine black powder (the CNC sample) was obtained after drying at 60 ºC under vacuum.

## Characterization

The TG studies were carried out using a NETZSCH TG 209F1 thermogravimetric analyzer. The crystal structure was characterized by X-ray diffraction (XRD, Bruker D8 Advance X-ray diffractometer) with high-intensity Cu-Kα radiation (λ=0.15406 nm). Scanning electron microscopy (FESEM, Hitachi S-4800, Hitachi Corp., Japan) and transmission electron microscopy (TEM, JEM-2100F) were used to observe the morphology. X-ray photoelectron spectroscopy (XPS) analysis was performed with an RBD-equipped PHI-5000C ESCA system (Perkin-Elmer Co., USA) using monochromatic Al Kα radiation (hν = 1486.6 eV). Raman spectra were recorded using a Raman spectrometer (InVia Reflex, Renishaw Corp., UK) coupled to a microscope in reflection mode with a 633 nm excitation laser source. The specific surface area was evaluated using the Brunauer-Emmett-Teller equation (BET) on a Tristar 3020 instrument (Micromeritics Corp., USA) at the temperature of liquid nitrogen. The pore size distribution was investigated using the Barrett-Joyner-Halenda (BJH) method derived from the desorption isotherm.

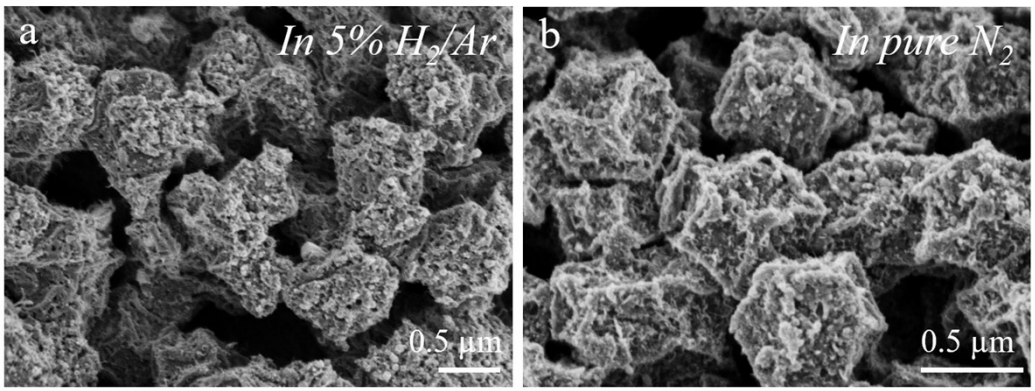


**Fig. S1** SEM images of NC-ZIFs after annealing in (a) 5% $H_2$/Ar mixed atmosphere and (b) pure $N_2$ atmosphere.

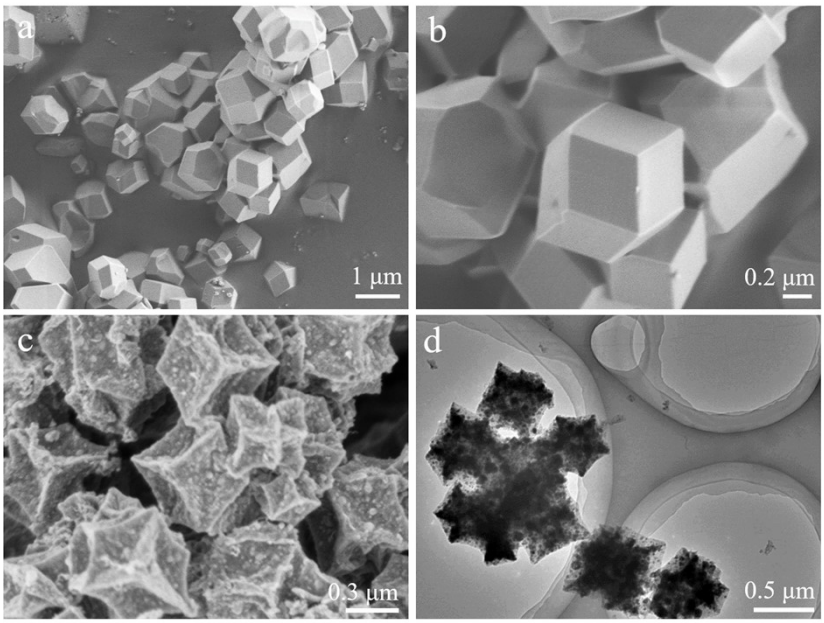


**Fig. S2** (a) Low- and (b) high-magnified FESEM images of ZIF-67; (c) FESEM image and (d) low TEM image of CNC sample, respectively.

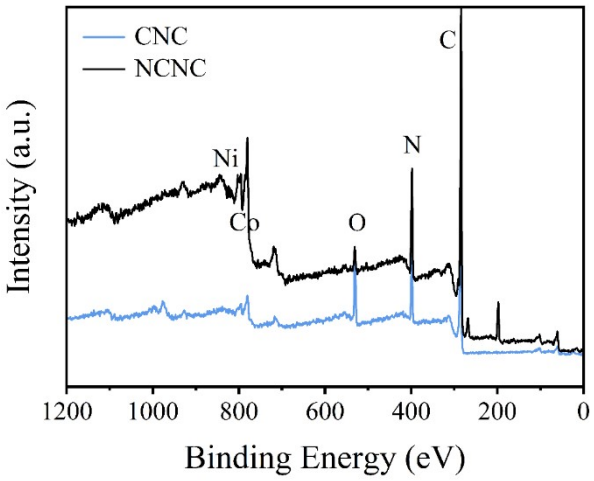


**Fig. S3** The XPS survey spectrum of NCNC and CNC catalysts.

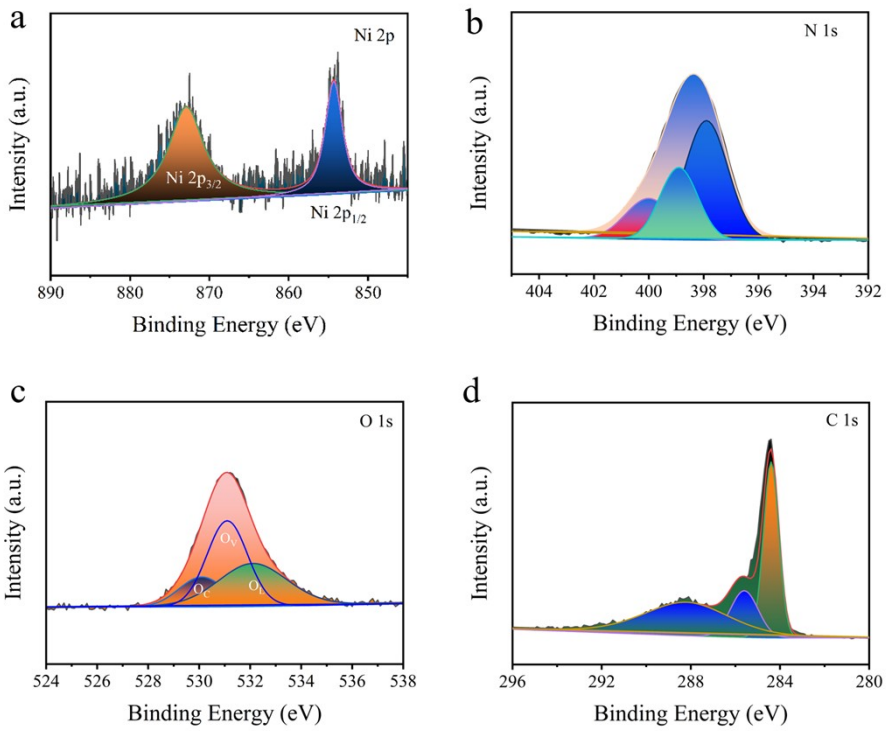


**Fig. S4** The high-resolution XPS spectra of (a) Ni 2p, (b) N 1s, (c) O 1s and (d) C 1s in NCNC catalyst, respectively.

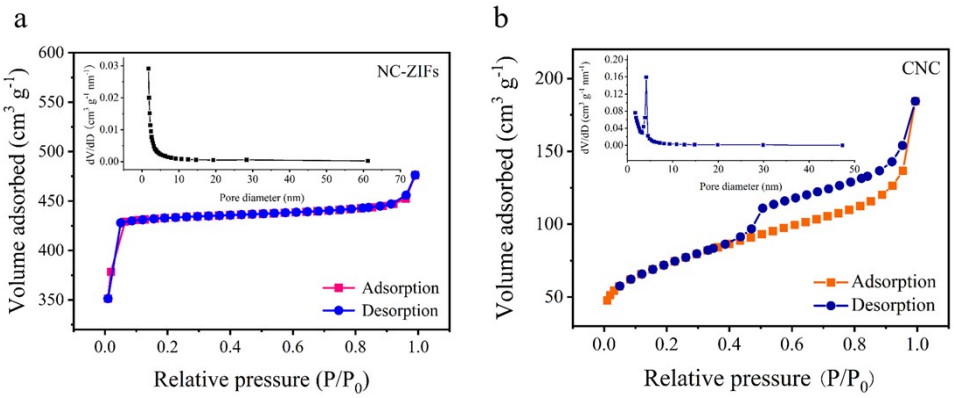


**Fig. S5** $N_2$ adsorption–desorption isotherms and pore-size distribution of (a) NC-ZIFs and (b) CNC sample, respectively.

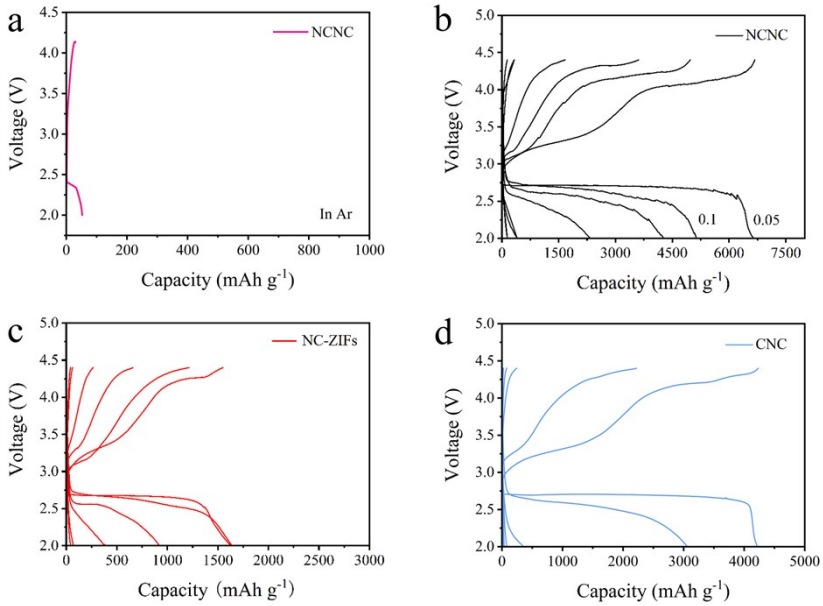


**Fig. S6** (a) the discharge-charge profiles at 0.05 mA $cm^{-2}$ of NCNC cathode-based cell in pure Ar; the rate performance of the discussed cathodes from 0.05 mA $cm^{-2}$ to 0.5 mA $cm^{-2}$: (b) NCNC, (c) NC-ZIFs, and (d) CNC cathodes.

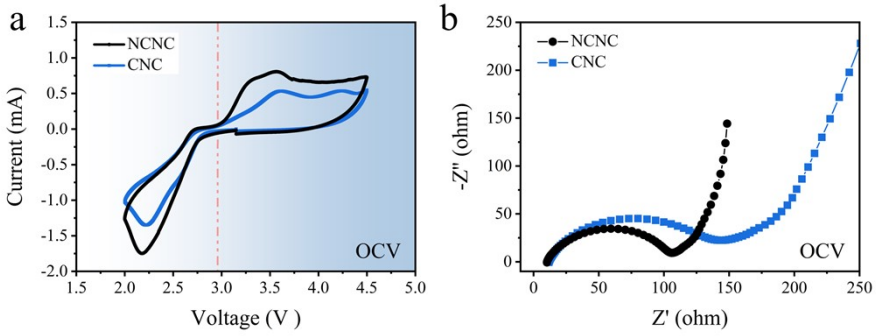


**Fig. S7** Electrochemical performance of NCNC and CNC cathodes. (a) CV curves at a scan rate of 0.5 mV/s and (b) Nyquist plots of the NCNC electrode (in black) and CNC electrode (in blue) before discharge.

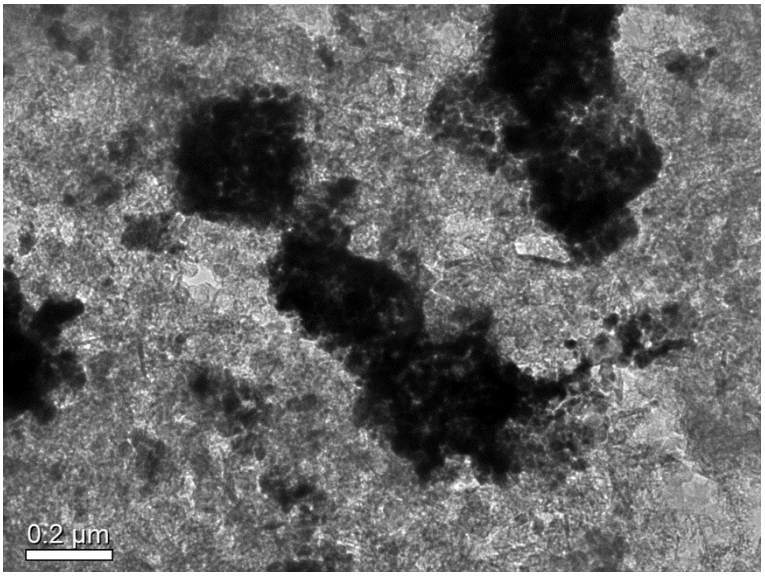


**Fig. S8** The TEM image of NCNC cathode after full discharge